Bull. Spec. Astrophys. Obs., 2000, 50, 91–103

A multielement array in the radio telescope focus

E.K. Majorova, V.B. Khaikin

Special Astrophysical Observatory of the Russian AS, Nizhnij Arkhyz 369167, Russia

Received March 14, 2000; accepted September 20, 2000.

Abstract. Performance data of radio telescopes with a multielement focal array are investigated. The problems of optimization of the array design, the elements of which are horizontally oriented strip radiators, are discussed with reference to RATAN-600 and a paraboloid of rotation. A computation of beam patterns of these telescopes operated in the mode of multibeam reception with the use of different modifications of focal arrays is performed. A "terrace-like" design of focal array for illumination of the non-symmetric secondary mirror of RATAN-600 and symmetric mirrors (paraboloids of rotation) is proposed.

Key words: radio telescope, focal array, multibeam reception

1. Introduction

The multibeam operation of a radiotelescope can be implemented by placing a matrix of primary feeds in its focal plane. This kind of multielement receiving array at the focus of a reflector radio telescope widens essentially its field of view, improves the integral sensitivity, speeds up the imaging of extended sources, reduces the influence of the atmosphere.

Receiving arrays in the form of matrix radiometers were used with the 12 m and 90 m radio telescopes at NRAO (Payne, 1988; Sutton, 1984). A 9-beam array for 21 cm has been in successful operation with the 64 m telescope at Parkes (Bird, 1994). A 32-element array in the range 85–112 GHz has been employed with the 14 m radio telescope at FCRAO (Erickson et al., 1992). A possibility of making a phased antenna array at the RATAN-600 focus is considered in the paper by Pinchuk et al. (1995). One of the alternative designs of a receiving array in the form of a matrix radiometer at the wavelength of 1 cm for the radio telescope RATAN-600 has been suggested by Berlin et al. (2000).

In the above-mentioned papers, waveguide horns with a specified level of illumination of the mirrors are used as the focal feed arrays with the use of strip radiators as has been proposed for a radio telescope by Smits, Smolders (1998) and Khaikin et al. (1998). Low loss substrate materials and Microwave Monolitic Integral Circuits (MMIC) developed during the few past years made strip arrays competitive for radio astronomical applications.

For the creation of a phased antenna array with an area of 1 km^2, wide band strip dipoles or Vivaldi radiators with a vertical orientation in space (Smits, Smolders, 1998) will be used in the SKA project. Khaikin et al. (1998) have proposed use of horizontally oriented microstrip radiators as being the most adaptable and providing the highest density of location of the elements. Optimum distribution of these radiators in the focal plane of the radio telescope will increase substantially the number of the array receiving elements.

In the present paper the question of optimization of the multielement focal array design with horizontally oriented strip radiators as applied to RATAN-600 and paraboloid of rotation is discussed, a calculation is presented of beam patterns (BP) of these telescopes in the multibeam reception mode with the use of different modifications of focal arrays.

2. The number of elements and the step of the receiving array in the focal region of the radio telescope

The optimum number of receiving elements at the focus of a radio telescope depends on the particular astrophysical task. For a rapid imaging of a sky region of $L_1 \times L_2$ in size the number of elements of the array must thus be equal to $N_1 \times N_2$, where $N_1 = L_1/\Delta L_1$, $N_2 = L_2/\Delta L_2$, ΔL_1, ΔL_2 are the array intervals equal to the half power beam width (HPBW) of the radio telescope in far zone in mutually perpendicular planes. For radio telescopes with a sufficiently large ratio $f/D \geq 1$ the beam pattern of a radio telescope in the far zone corresponds to the field distribution at the focus. In accordance with the sampling theorem for the power signal, we have: $\Delta L = 0.5\lambda f/D$, where f is the focal length, D is the aperture diameter, λ is the wavelength. The size $L_1 \times L_2$ and the field of view are practically limited by the size of the

aberration-free zone L_a in the focal plane, which determines a possible N as $N = (L_a/\Delta L)^2$ in the case the telescope is symmetric.

In the case where the multibeam mode is used to perform the task of improving the integral sensitivity of the radio telescope, one seeks to reach a possibly larger number of independent receiving elements through their denser placing, up to $\Delta L = \lambda_s/2$, where λ_s is the wavelength at the substrate of a strip element, which is in inverse proportion to $\sqrt{\varepsilon}$ ($\varepsilon > 1$), ε is the dielectric constant for ϵ of the substrate material. However, the denser disposition of elements results in reduction of sensitivity of each element. Besides, the noise in the neighbouring receiving channels becomes partially correlated. For these two reasons it is a failure to reach the desired factor of $\sqrt{N_{max}} = \sqrt{(2\Delta L/\lambda_s)}$. The step of the array is therefore usually bounded above by the sampling Nyquist theorem and below by the geometric structure of radiators and by the permissible mutual coupling between them (usually one seeks to reach coupling between the elements not less than -30 dB).

It is well known that the two-beam scanning reduces the effect the atmosphere has on the telescope performance. Subtraction of the output signals of separated elements of the receiving array may also be effective enough to control atmospheric fluctuations. Pairs of elements with a maximum separation in the focal region $N\Delta L/2$ will yield the largest angular scale S of the supressed atmospheric fluctuations:

$$S = 0.5N\Delta L/f.$$

Note the advantages of the multibeam operation of a radio telescope in controling atmospheric fluctuations over the two-beam one. In the multibeam mode, residual atmospheric fluctuations in neighbouring pairs of beams are correlated and can be removed.

3. A one-dimensional array at the focus of RATAN-600

Depending on the condition of observations, the antenna of the radio telescope RATAN-600 is a two- or three-mirror focusing system (Khaikin et al., 1972). In the case of two-mirror system a flat wave from a cosmic object, when striking the aperture of the main mirror (circular reflector), is transformed by the latter into a cylindrical one. The reflecting elements of the main mirror form a focusing surface that represents a fraction of an elliptical cone, at the focus of which a secondary mirror is placed which convert a cylindrical wave to a spherical one. The latter is received by the receiving horn (primary feed) located at the focus of the secondary mirror (Fig. 1). This is the pattern of operation of the North, West, South and East sectors of RATAN-600. Observations are made in the mode of a source transit across the stable BP of the radio telescope. The focusing of the radio telescope beam in a given direction is executed by changing the shape of the main mirror surface and the position of the secondary mirror on the rails.

The South sector together with the flat periscopic mirror form the three-mirror system similar to that of Kraus in Nancay. The flat mirror changes the direction of the plane wave from a source, which after reflection is redirected to the main mirror. Further the focusing of beams is accomplished in the same manner as with the two-mirror system. In the three-mirror system the shape of the main mirror, which is a parabolic cylinder with a vertical generant, does not change with elevation of the source. The BP is controlled by way of changing the inclination angle of the flat reflector panels. The secondary mirror is a non-symmetric parabolic cylinder with a horizontal generant, on the focal line of which (X axis in Fig.1b) primary feed cabins are located, which enables simultaneous observations at several wavelengths. This design of the secondary mirror is convenient for the multibeam mode of operation of the radio telescope with the one-dimensional array (Kajdanovskij, 1980).

The number of elements in the array is determined by the size of the aberration-free zone of the radio telescope, which, under the condition of two-mirror focusing system of RATAN-600, depends on the elevation of the source being observed. Korzhavin (1979) and Esepkina et al. (1980, 1982) considered in some detail the aberrations arising when the primary feed is removed from the focus, derived formulae for calculation of BP and studied polarization characteristics of RATAN-600 with allowance for aberrations. Basing on these papers and using the programmes kindly made available to us by A.N. Korzhavin, we have computed the BP of the radio telescope for the main and spurious polarizations with different removals of the primary feed from the focus along the X axis and plotted aberration curves of the radio telescope in the case of two-mirror focusing system. By the aberration curves we mean the relationships between the maximum of the telescope BP, F_{max}, and the removal of the primary feed from the focus.

Examples of the two-dimensional power BP of RATAN-600 at the wavelength 10 mm for the focused antenna (a) and with the primary feed removed from the focus by 1000 mm along the X-axis (b) for the source elevation $H = 85°$ are displayed in Fig. 2. Figs. 3 and 4 present the BP of the circular and linear spurious polarizations when receiving unpolarized radiation, which are characterized by Muller matrices M41 and M32, respectively ((a) with $\Delta x = 0$ mm, (b) with $\Delta x = 1000$ mm). The aberration curves for the main $F_{max}(\Delta x)$ (a) and spurious $M41_{max}(\Delta x)$, $M32_{max}(\Delta x)$ (b) polarizations are pre-

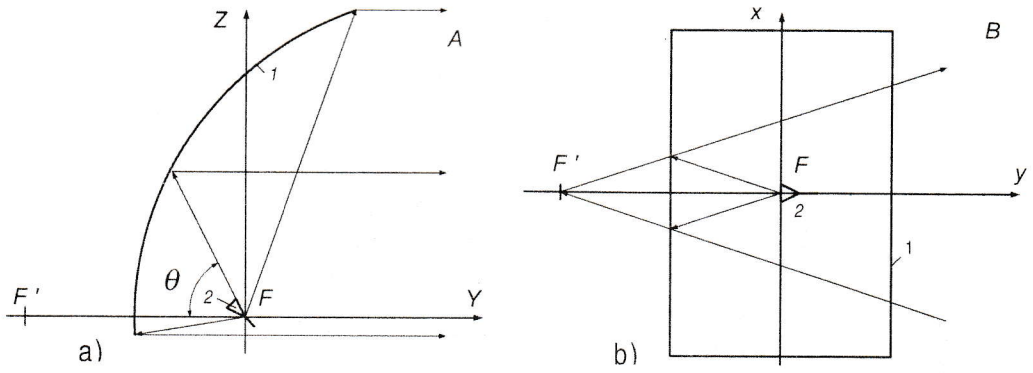

Figure 1: *The section of the secondary mirror in the vertical (a) and horizontal (b) planes. 1 — the parabolic mirror, 2 — the primary feed.*

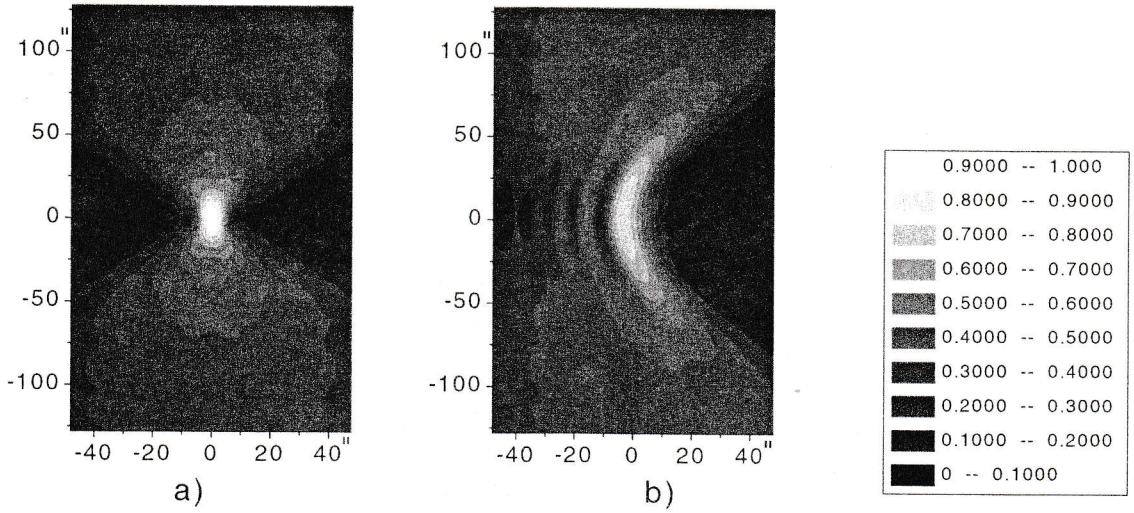

Figure 2: *The two-dimensional power BP of RATAN-600 (principal polarization) at the wave of 10 mm at* $H = 85°$. *(a)* — $\Delta x = 0$ *mm, (b)* — $\Delta x = 1000$ *mm.*

sented in Figs. 5, 6.

As one can see from Figs. 5, 6 the one-dimensional array placed on the focal line of the secondary mirror is the most efficient when observing sources with altitude close to 90°, since under this condition the aberration-free zone of RATAN-600 is maximum. With decreasing altitude of the source, the aberration-free zone narrows rapidly. The aberration-free zone size at the wavelength 10 mm is about 3 m (curves 1 and 2 in Fig. 6a) near the zenith, while for the height $H = 0°$ a signal drop in the main polarization by no more than 20% can be provided only with removal of the primary feed from the focus by $\Delta x = \pm 25$ mm (curve 1 in Fig. 5a). The number of strip radiators in the one-dimensional focal array at the wavelength 10 mm in observing near-zenith sources may thus be 500 elements, whereas for effective reception of radiation from low elevation sources their number should not be larger than 10.

As to the spurious polarization, it is minimum at altitudes close to zero and grows monotonically with increasing altitude of the source. For this reason, in polarization measurement the three-mirror focusing system of RATAN-600 with the periscopic flat mirror ("South+Flat" mode), in which the circular mirror is set vertically to the altitude H=0°, appears to be more preferable.

Fig. 6a shows also an aberration curve (3) of the radio telescope RATAN-600 in the mode "radio-Schmidt telescope" for a certain fixed source altitude to which the system was designed and the horizontal size of the aperture of 100 m. The shape of the aberration curve remains unchanged with changing altitude of the source in the range of angles 0° to 90°, provided that the source altitude and the altitude to which the focusing of the antenna was performed coincide.

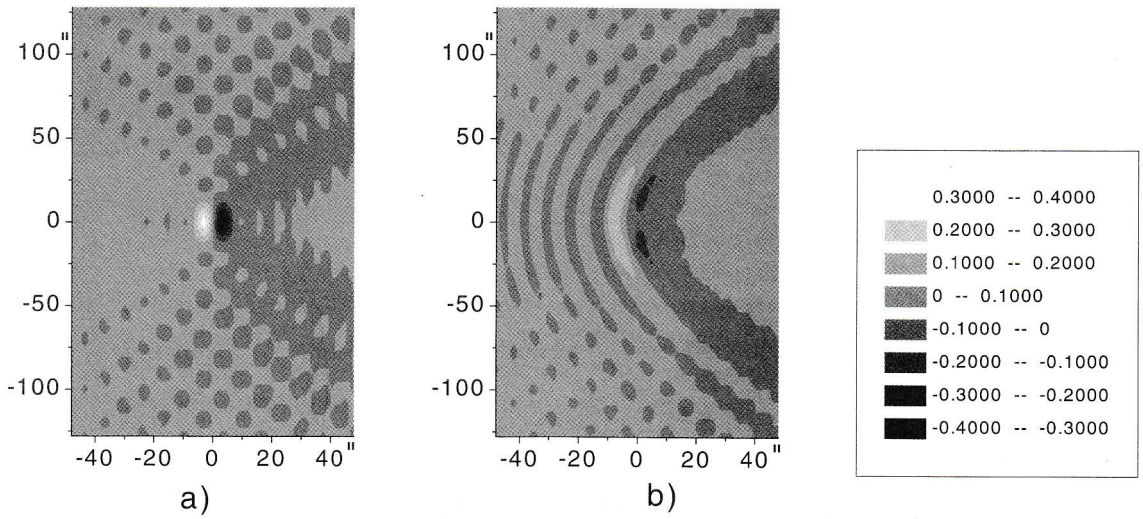

Figure 3: *The BP of the circular spurious polarization (the element of the Muller matrix M41) at the wavelength 10 mm at $H = 85°$. (a) — $\Delta x = 0$ mm, (b) — $\Delta x = 1000$ mm.*

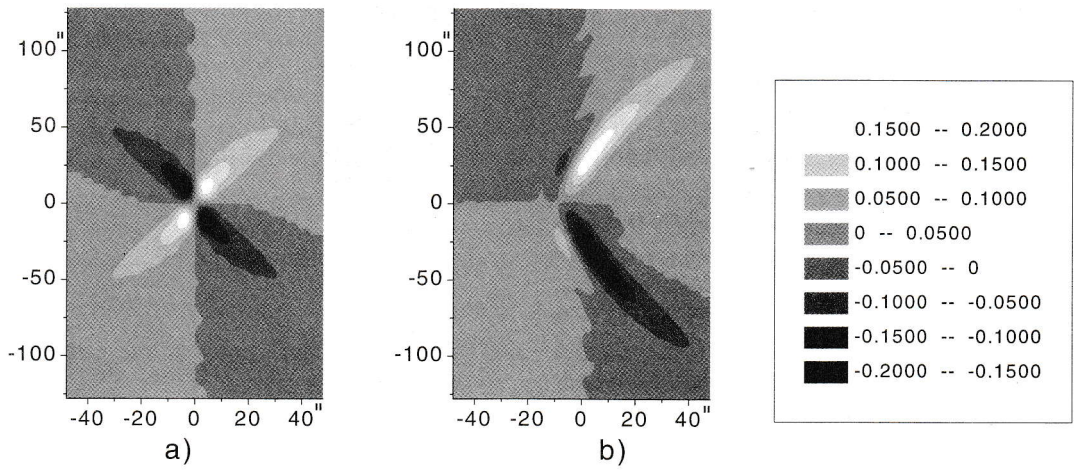

Figure 4: *The BP of the linear spurious polarization (the element of the Muller matrix M32) at the wavelength 10 mm at $H = 85°$. (a) — $\Delta x = 0$ mm, (b) — $\Delta x = 1000$ mm.*

The radio-Schmidt telescope mode can be implemented by shaping the periscopic mirror to a required curvature to correct the wave front (Majorova, Khaikin, 1999). The largest size of the aberration-free zone and the least curvature of the field in the focal plain can be achieved in the particular case of the radio-Schmidt telescope, when the focus of the system is located near the correcting mirror. In optics, such a system is called shortened Schmidt telescope or Right telescope. With RATAN-600 this mode is implemented by placing the secondary mirror near the periscopic reflector executing correction of the wave front.

As can be seen from Fig. 6a, the aberration curve in the condition of the "radio-Schmidt telescope" is practically coincident with those of the two-mirror focusing system at high elevation angles, therefore the maximum number of elements of the array in this mode at 10 mm may also reach 500 elements. The advantage of the "radio-Schmidt telescope" is that it makes use of a wide aberration-free zone not only near the zenith, but also at any other angle within the range $0° - 90°$. The disadvantage is the reduction of the aperture and the limitation on the range of ob-

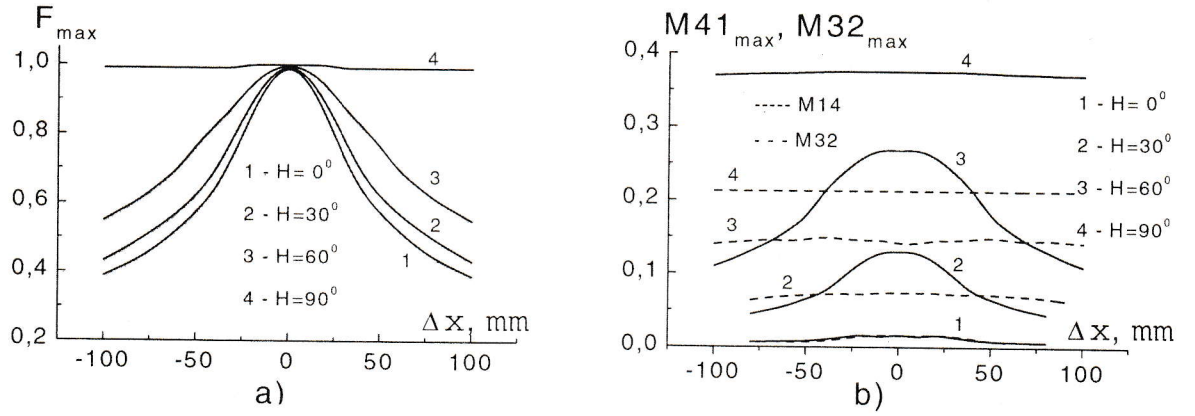

Figure 5: *The aberration curves at the wavelength 10 mm with the removal of the primary feed along the focal line of the secondary mirror (X axis). The regime of the two-mirror focusing system with the full aperture.*

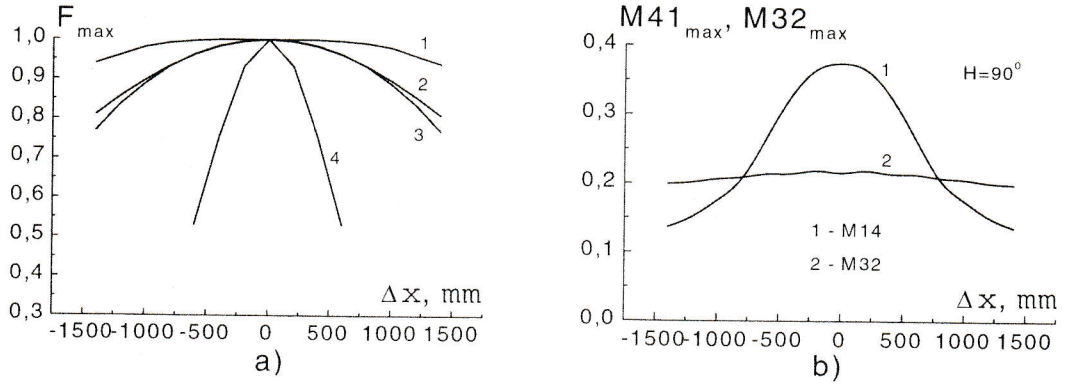

Figure 6: *The aberration curves at the wavelength 10 mm with the removal of the primary feed along the focal line of the secondary mirror (X axis). 1 — $H = 90°$, 2 — $H = 89°$, 3 — "radio-Schmidt" telescope, 4 — $H = 0°$; 1, 2 — full aperture, 3, 4 — shortened aperture.*

serving angles with the given focusing of the antenna (Majorova, Khaikin, 1999).

It should be noted that the reduction of the aperture results in an increase of the aberration-free zone also in the normal operation mode of the radio telescope, which is of particular importance at low elevation angles, but not as much important as with the "radio-Schmidt telescope" mode. For comparison, Fig. 6a displays an aberration curve in the condition of two-mirror focusing system at the wavelength of 10 mm for the 100 m aperture and $H = 0°$ (curve 4). It is seen that with equal sizes of the apertures and observing angles the aberration-free zone in this mode is much more narrow than in the "radio-Schmidt telescope" mode.

4. Two- and three-dimensional arrays at the focus of RATAN-600

Let us dwell upon the distinguishing features of the BP of RATAN-600 in the condition of two-mirror focusing system. Note that the BPs displayed in Figs. 2, 3 and 4 were calculated in an approximation of an infinitesimal vertical size of the reflecting element (panel) of the main mirror. Its influence with the considered transverse removals of the primary feed from the focus at altitudes close to 90° is insignificant. It is shown in the paper by Esepkina et al. (1961) that with allowance made for the finite size of the panel the BP of RATAN-600 can be represented as the product of two BPs: the BP of the focusing system in the form of an infinitely thin arc in aperture plane and that of an individual panel. In a different way, the BP of RATAN-600 is the BP of the focusing system with the panel envelope superimposed on it.

The width of the main lobe of the vertical BP of the focusing system is determined by the aperture curvature, or the depth of the arch reflecting the aperture curvature, the width of the envelope — by the vertical size of the panel with allowance for its illumination in the vertical plane. At altitude close to 90° the HPBW of the main lobe of the vertical BP of

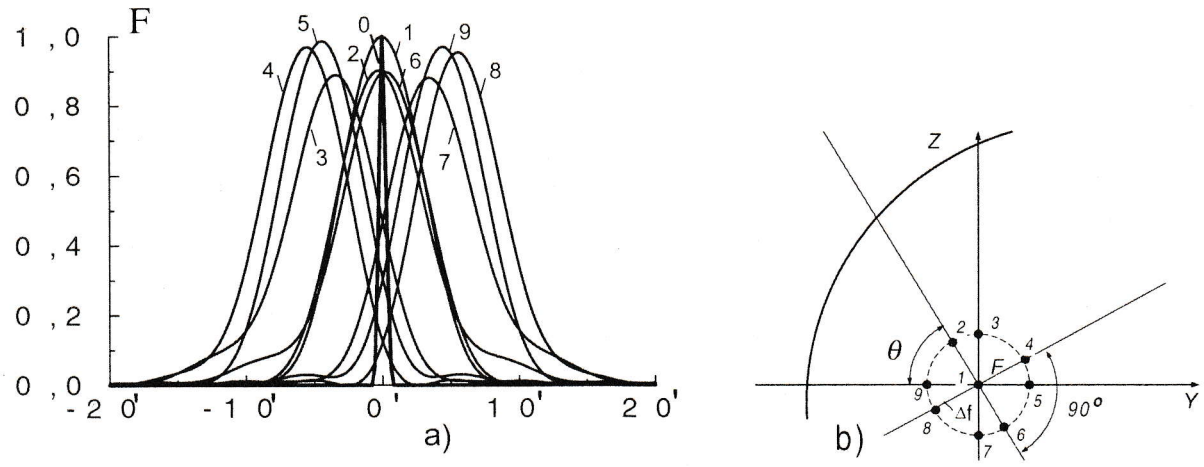

Figure 7: *The vertical BP of the panel* $(1 \div 9)$ *at the wave of 10 mm with location of the primary feed at a fixed distance from the focus and the BP of the focusing system (0) for* $H = 85°$ *(a). The schematic view of location of feeds in the vertical section of the secondary mirror at points* $1 \div 9$ *(b).*

the focusing system is an order of magnitude smaller than the HPBW of the panel BP. As the altitude of the source decreases, the width of the BP of the focusing system increases, approaching the BP of the panel at low elevation angles. At $H = 0°$ the vertical BP of the radio telescope coincides with that of the reflecting element.

Under the condition of the focusing system "South+Flat" the vertical beam pattern of RATAN-600 coincides with the vertical BP of the panel for any altitudes of the source being observed in the range $0° - 90°$.

To assess the possibility of using two- and three-dimensional arrays in the focal region of RATAN-600, calculations of the vertical BP of the panel were carried out with arbitrary removal of the primary feed from the focus F on the plane A (Fig. 1a). The programmes of A.N. Korzhavin, which took account of all geometrical features of the secondary mirror and allowed calculation of the field distribution over its aperture, proceeding from the BP of the primary feed, were used (Korzhavin, 1979).

Curves 1–9 in Fig. 7a show the vertical BP of the panel at the wave of 10 mm with a removal of the primary feed from the focus by $\Delta f = 5$ mm and locating it at points 1, 2, 3, 4, 5, 6, 7, 8, 9, (Fig. 7b). Points 2 and 6 correspond to feed removals along the direction $\theta = 50°$, points 4 and 8 — to removal perpendicular to this direction. The beam patterns of the primary feeds and the real sizes of the focusing system of RATAN-600 were specified in the calculation. It was assumed that in each of the locations the maximum of the primary feed BP makes an angle $\theta = 50°$ with the horizon. In this case, optimum illumination of the secondary mirror is provided.

Curves 1–9 in Fig. 7a are the envelopes of the BP of the radio telescope in the mode of the two-mirror focusing system at $H \neq 0°$. The bold line (0) in the figure shows the vertical BP of the focusing system at $H = 85°$. It is obvious that if the maxima of the BPs of the panel and focusing system are largely separated, a sharp signal drop will occur. In order that it should not take place, the elements of the two-dimensional array have to be arranged in the vertical plane along the direction $\theta = 50°$ (points 2, 1, 6 in Fig. 7b). But it is this case that cannot be practically implemented because the feeds shade each other in the direction of illumination. For this reason, under the condition of the two-mirror focusing system at $H \neq 0°$, the use of the two-dimensional array appears to be impossible. Later on, when studying the configuration and sizes of the two-dimensional array, we will consider the regime of the three-mirror antenna system of RATAN-600, for which the vertical BP of the focusing system coincides with the panel BP.

It can be seen from the curves given in Fig. 7a that for obtaining a maximum signal the arrangement of the array elements along the Y axis or along the direction perpendicular to the direction $\theta = 50°$ is preferable. In this case the maximum of radiation of individual elements of the array must make an agle of 50° with the horizon. In the case where the horns or the open ends of the waveguides are the primary radiators, it presents no problem to specify this direction in the two cases indicated above. For a flat array, which is a matrix of horizontally oreiented strip feeds, whose maxima of radiation are perpendicular to the array plane, the arrangement of the elements along the Y axis is impossible because practically all the

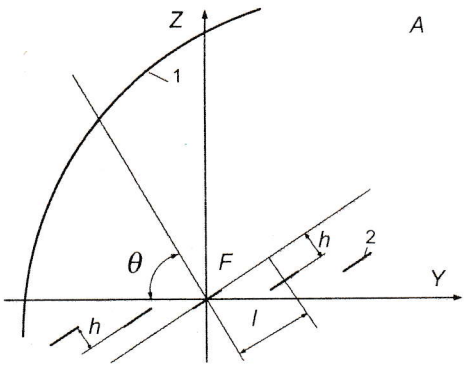

Figure 8: *The schematic view of the "terrace" arrangement of the primary radiators in the focal region of the secondary mirror of RATAN-600 (vertical section). 1 — the parabolic mirror, 2 — the fences of the primary radiators.*

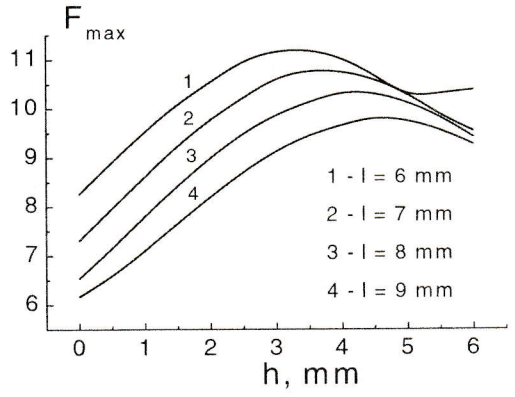

Figure 9: *The relationship between the maximum of the RATAN-600 BP in the "South–Flat" operation with the "terrace" array in its focal region and parameters of the array l and h.*

radiation will bypass around the surface of the secondary mirror. The most optimum for such an array is the location of the radiators in a plane perpendicular to the direction $\theta = 0°$. As calculations have shown the deviation from this direction must not be more than $\pm 5°$.

The next step of our study is the examination of a three-dimensional array consisting of linear strip arrays (LSA) of radiators. These fences are parallel to the focal line of the secondary mirror and shifted with respect to each other in the vertical plane by a value h, the distance between the radiators in the fences is set by the parameter l (Fig. 8). Let us name this setup "terrace".

Compute the relations between the maximum of the antenna BP, F_{max}, in the "South+Flat" mode and the distances h and l. They show (Fig. 9) that for each of the considered values of the parameter l there exists an optimum value of h_{opt} with which $F_{max}(h)$ has a maximum value. h_{opt} is not equal to zero and, therefore, the location of radiators in one plane is not optimum. As can be seen from Fig. 9, for the practically real distances between the elements of the array, $l = 0.6 - 0.7\lambda$ (6–7 mm for the wave of 10 mm), the optimum shift of the fences in the array is $h = 0.3 - 0.4\lambda$ (3–4 mm). In further calculations we will assume $h = 3$ mm as the most optimum, however it has so far been managed to realize a shift of 4–5 mm between the fences with a separation of elements of 7–8 mm (Khaikin et al., 2000).

Fig. 10 presents the vertical beam patterns of the radio telescope RATAN-600 in the operation mode "South + Flat" in the central section at the wave 10 mm with location in its focal region of a receiving array of "terrace" design with parameters ($l = 7$ mm, $h = 3$ mm) — (a), and with the use of the array of flat design ($l = 7$ mm, $h = 0$ mm) — (b). The plane of the latter is perpendicular to the direction $\theta = 50°$. It is well seen that with the use of the "terrace" design the drop in the maxima of the BP of individual beams is less than with the flat design. With the same separation of the elements and their number ($N = 7$) the drop in signal in the marginal elements of the array amounts to about 40% in the case of the flat array, while for the "terrace" array it is no more than 15%.

Examples of the receiving array of "terrace" design with microstrip (patch type) radiators and MMIC amplifiers are shown in Fig. 11. Such a design is not only more simple in realization, but also turns out to be more optimum in energy characteristics. Mutual influence of the elements in the "terrace" design is lower comparing to the flat array (Khaikin et al., 2000).

The optimum number of LSA in the "terrace" receiving array for RATAN-600 is 7–8. Under the condition of the three-mirror focusing system irrespective of the source altitude and in the mode of the two-mirror focusing system at altitudes close to 0°, with allowance made for the aberration curve 1 in Fig. 5, along the focal line of RATAN-600 each LSA can hold no more than 10 elements. Thus, in these modes of the radio telescope operation one can implement multibeam observations with the two-dimensional "terrace" array with a total number of receiving elements of about 70.

In the mode of the "radio-Schmidt" telescope, where the aberration-free zone is substantially larger (curve 3 in Fig. 6), the number of elements in the three-dimensional array may reach 3000. Observations can be made at any fixed source altitude, provided that it coincides with the altitude the "radio-Schmidt" is designed for, with an antenna aperture size no more than 150 m.

Implementation of a data acquisition system (DAS) with such a number of elements is rather a

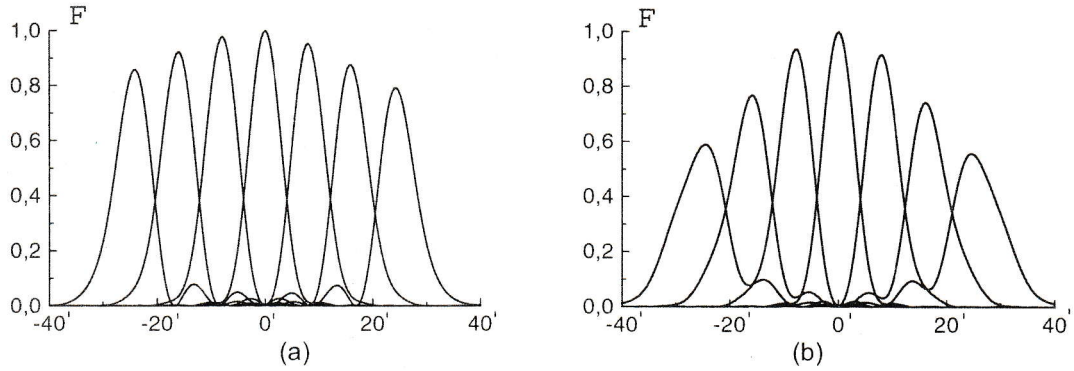

Figure 10: *The vertical BP of the radio telescope RATAN-600 under the condition "South + Flat" at the wave of 10 mm with location in its focal region of the receiving array of "terrace" (a) and flat (b) design.*

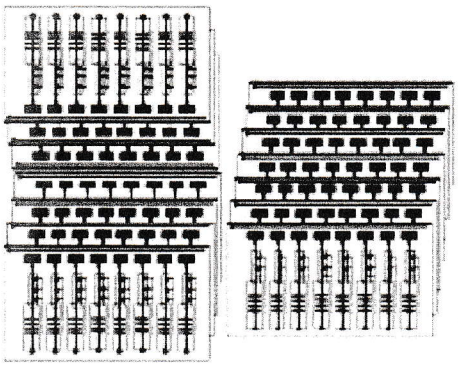

Figure 11: *The examples of "terrace" design of the multielement receiving array with microstrip (patch) radiators and MMIC amplifiers.*

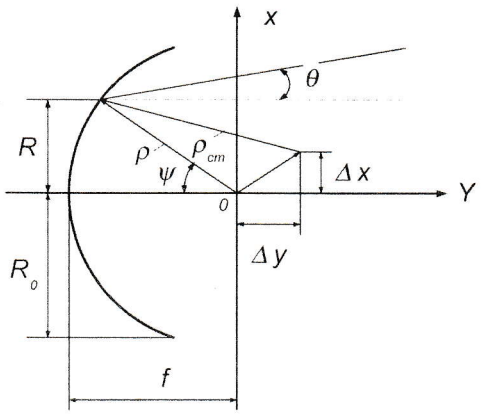

Figure 12: *The paraboloid schematic view.*

complicated but feasable task. One of the alternatives of a 16-channel DAS with a digital signal processor (DSP) for a multielement array is proposed by Esepkina et al. (2000).

We will note in conclusion that the results obtained for the RATAN-600 can be used for to the general case of radio telescopes with non-symmetric illumination for which the "terrace" design of the focal multielement array will also be more favoured.

5. A multielement array at the focus of a paraboloid

Now we will consider the case of a parabolic radio telescope with symmetric illumination. To provide a multibeam mode of operation of a parabolic radio telescope, a matrix of primary feeds is placed in the focal plane. It follows from the focusing properties of a paraboloid of rotation that the disposition of the primary feeds in which their phase centres lie in the same plane is considered optimum. However, construction of a flat strip array entails difficulties (Khaikin et al., 2000). For this reason, we consider the possibility of "terrace" construction of the receiving strip array as applied to paraboloids.

Let us compute the BP of a parabolic antenna with an arbitrary removal of the feed from the focus $\Delta f = \sqrt{(\Delta x)^2 + (\Delta y)^2}$ (Fig. 12).

The expression for the BP has the form:

$$F(\theta, \delta) = \int_0^{2\pi} \int_0^{R_0} E(R/R_0) e^{j\beta R \sin\theta \cos(\delta - \varphi) + j\beta\Phi} \, R \, dR \, d\varphi$$

where
$\Phi = \rho_{cm} - \rho = \sqrt{(\rho\cos\psi + \Delta y)^2 + (\rho\sin\psi - \Delta x)^2}$,
θ, δ are the coordinates of the point of reception, Δx is the removal from the focus along the X axis, Δy is the removal along the Y axis, $E(R/R_0)$ is the field distribution over the antenna aperture.

Taking account of axial symmetry of a paraboloid, we restrict ourselves to a consideration of the BP in one of its radial section, $X0Y$, at $\delta = 0$. The BP computation was performed by the method of numerical integration. The field distribution in the aperture was specified by the law $E(R/R_0) = 1 - (R/R_0)^2$, f/D

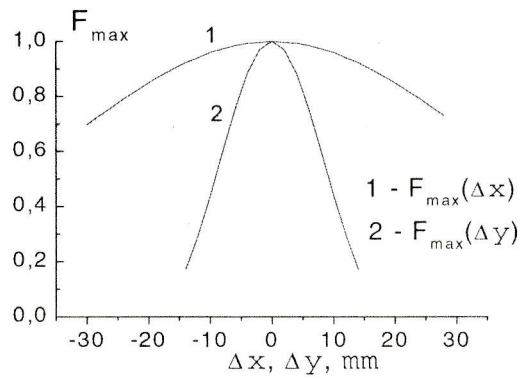

Figure 13: *The aberration curves for a paraboloid of rotation with $f/D = 0.4$ at the wavelength 10 mm with removal of the primary feed from the focus in transversal (1) and longitudinal (2) directions.*

$=0.4$, $\lambda = 10$ mm.

Fig. 13 shows aberration curves for a paraboloid of rotation with removal of the primary feed from the focus in the longitudinal (along the Y axis) and transverse (along the X axis) directions. The curves characterize the appearance of root-mean-square and cube errors in removal of the feed in the directions X and Y, respectively.

Fig. 14 displays examples of "terrace" construction of the array, which take account of axial symmetry of the paraboloid (circular variant). The location of the radiators is shown in one of the radial sections of the paraboloid — in the plane that passes through the radius of the circle, which is the aperture of the paraboloid and its axis of symmetry (a), and in the frontal section — in the plane perpendicular to the paraboloid axis (b). In this design the radiators are arranged in rings shifted with respect to each other in depth by the quantity h. The disposition is shown of both the even and odd number of radiators in the radial section of the paraboloid.

Fig. 15 exhibits the beam patterns of the parabolic antenna in the focal plane of which strip radiators are placed, which form a "terrace" array in its circular version (Fig. 14). N is the number of array elements in each of the radial sections. The beam patterns were calculated for the sizes $h = 3.1$ mm and $l = 5.3$ mm, which are the most optimum. The position of the array, as a rigid structure, with respect to the paraboloid focus was optimized in each of the cases considered in such a way that the aberrations were minimum with specified h and l.

As can be seen from the figures, the use of the "terrace" design when creating the array is not only possible, but for the cases where $N = 3, 4$ it gives an advantage over the ordinary flat design. With $N = 3, 4$ an equal signal level is attained in all beams of the paraboloid BP, which cannot be achieved with the flat design. When the latter is in use, the variation of maxima of individual beams of the BP will occur in correspondence with aberration curve 1 in Fig. 13.

Apart from the axially symmetric array construction, rectangular designs shown in Fig. 16 are possible. The LSA of the radiators are shifted by h, and the location of the radiators in this plane is the same as in Fig. 14a. The BP in this section will coincide with the BP of the axially symmetric array in its radial section (Fig. 15): completely for the odd number of elements N and to an accuracy of a few per cent for the even. The shape of the multibeam BP of the paraboloid in the plane $(Y0Z)$ will change (Fig. 17). The maxima of the BP of individual beams will decrease monotonically as the radiators are moved away from the focus of the radio telescope.

The "terrace" design of the array is thus quite suitable for paraboloids and, in some cases, has even certain advantages over the flat array. Axially symmetric circular designs with a number of elements of 7×7 or 8×8, shown in Fig. 14, can be used in the focal region of parabolic mirrors in a range up to 30 GHz.

6. Some radio astronomy applications of the multielement focal array

A multielement array in the focus of a radio telescope can be used to perform a wide range of tasks in radio astronomy. The application of focal arrays is inavitable for present-day and future radio telescopes in high-accuracy and high-speed surveys (Parijskij et al., 1998).

This technique used at RATAN-600 improves significantly the integral sensitivity, widens the field of view, and controls effectively atmospheric fluctuations in studying anisotropy of the cosmic microwave background (CMB) on subdegree scales. Advantageous use of the focal array can be achieved by both the considerably growing amount of recorded information during the intervals of "good" atmosphere and additional possibilities of cleaning atmospheric interferences when the atmosphere is "bad".

A search for Syunyaev-Zeldovich (SZ) effect with a high spatial resolution and high sensitivity in brightness temperature can be carried out with RATAN-600 in the multibeam mode even with a reduced antenna aperture. In the case of realization of the average fluctuational sensitivity of one receiving channel at a level of 5–10 mK (which is achievable today with "warm" low noise MMIC amplifiers), the integral sensitivity of the radio telescope with the multielement focal array rises by more than an order of magnitude.

The multielement focal array will improve considerably the efficiency of RATAN-600 and other radio telescopes in the study of rapidly variable cosmic objects, such as pulsars and the Sun. Fig. 18 shows the

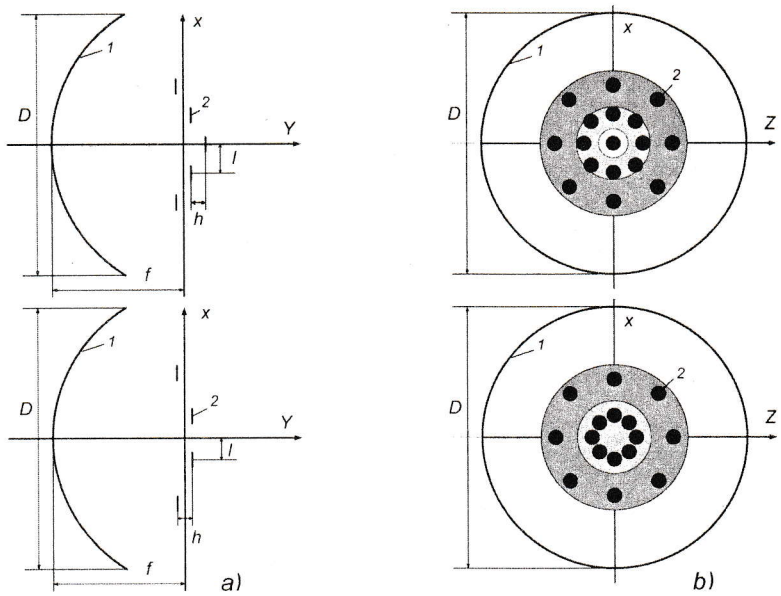

Figure 14: *The diagram of the "terrace" design of the array in the focal range of a paraboloid (circular alternative) in the radial section (a), in the frontal section (b). 1 — the paraboloid, 2 — the primary radiators.*

Sun with corona in the field of view of RATAN-600 in the mode "radio-Schmidt" telescope with a focal array of 7 × 170 elements at the 1 cm wavelength (left) and in the field of view of a 12 m parabolic mirror with an array of 8 × 8 elements at the 2 cm wavelength (right). So wide field of view with a high spatial and time resolution opens up new possibilities in the study of flares, microbursts and other rapid, but rare events on the Sun.

The equivalent spatial resolution, achieved with the use of the focal array in some cases, can be higher than HPBW owing to the increased signal-to-noise ratio and to simultaneous analysis of the signal from the source in different channels. An appropriate procedure for observations of flares on the Sun was developed by Herrmann et al. (1992).

One more possible application of focal arrays is holographic control of the surface of a radio telescope. An 8 × 8 element array, for instance, reduces significantly the time needed for measuring and subsequent holographic correction of surface errors with the help of a strong cosmic source or a satellite signal. This will be a powerful incentive to the development of methods of "adaptive optics" at radio telescopes, including the wave front correction.

7. Conclusions

The investigations carried out have shown that arrays with microstrip radiators can be used advantageously to implement the multibeam mode of operation of radio telescopes of different design.

For the radio telescope RATAN-600 a one-dimensional, two-dimensional and three-dimensional arrays can be employed. The first variant, in the form of LSA of radiators arranged along the focal line of the secondary mirror, is the most efficient in observing near-zenith sources and also in the regime of the "radio-Schmidt" telescope (with an arbitrary fixed altitude of the source being observed). The number of elements of such an array may reach 500 at the 10 mm wavelength.

The two- and three-dimensional variants of arrays can be implemented in the mode of the three-mirror focusing system of RATAN-600 (the "South + Flat" mode) at altitudes from 0° to 90° and in the mode of the two-mirror focusing system at $H = 0°$. The maximum number of elements of this array may reach 70 at the 10 mm wavelength. The use of the two-dimensional array in the regime of the "radio-Schmidt" telescope will allow the number of element to be increased to 3000, but with the reduced horizontal aperture of the antenna.

A possibility of non-flat disposition of the strip radiators in the focal region of the radio telescope is considered. A "terrace" design of the focal array for illumination of the secondary mirror of RATAN-600 is considered and its parameters are optimized. Calculations have shown that the use of arrays of "terrace" design in the focal region of non-symmetric feeds, which is the secondary mirror of RATAN-600, is more effective in energy characteristics, besides they are more simple in implementation as compared with flat designs, where horisontally oriented strip radiators are used as the array elements. Results of the calculations made in this paper were used in designing

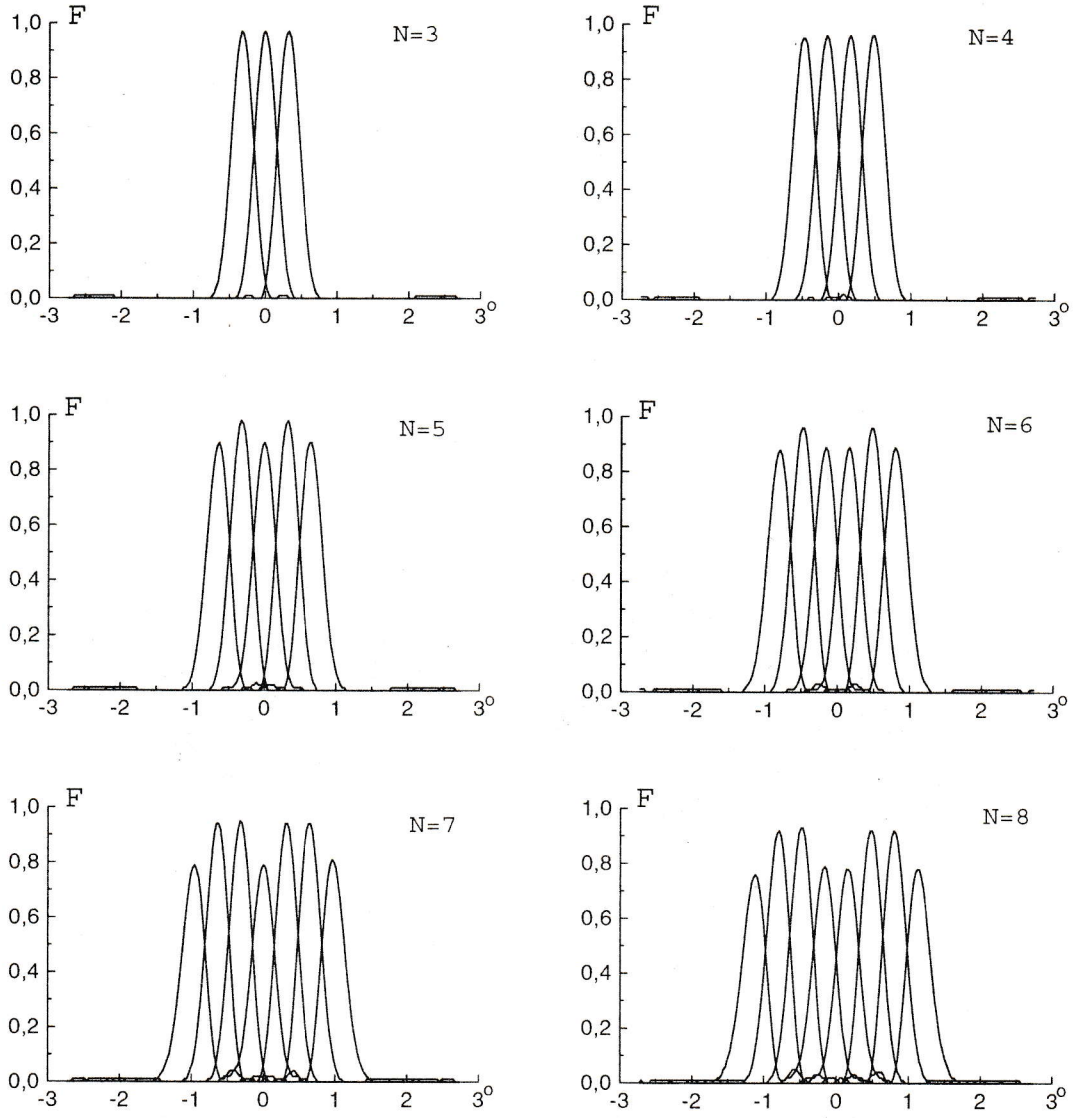

Figure 15: *The BP of a parabolic radio telescope at the 10 mm wave with a "terrace" array (circular alternative) placed in its focal region. N is the number of elements in the radial section.*

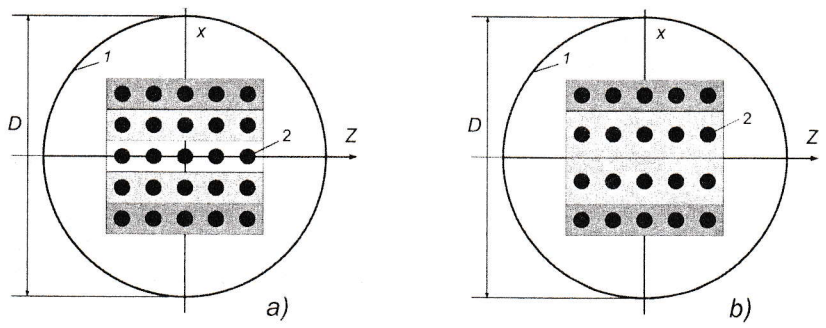

Figure 16: *The schematic view of the "terrace" array (rectangular alternative) in the focal region of a paraboloid, 1 — the paraboloid, 2 — the primary radiators.*

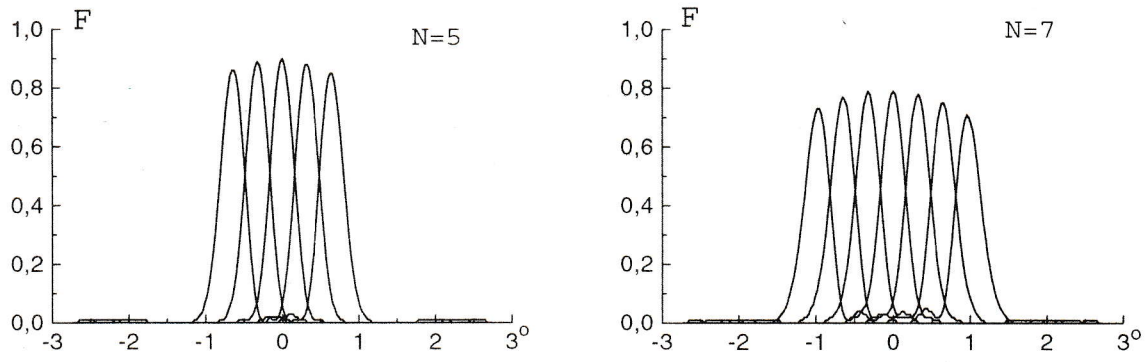

Figure 17: *The BP of a parabolic radio telescope at the 10 mm wavelength in the YOZ with the "terrace" array (rectangular variant) placed in its focal region.*

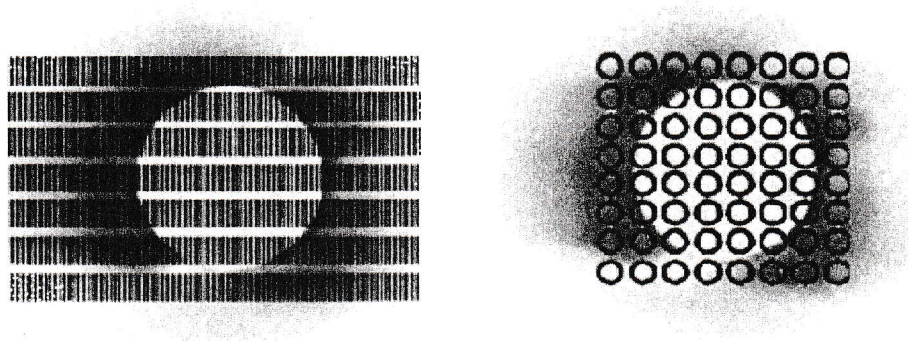

Figure 18: *The Sun with the corona in the field of view of RATAN-600 operated as the "radio-Schmidt" telescope at the 1 cm wavelength with a focal array of* 7×170 *elements (left) and in the field of view of a 12 m parabolic mirror with an array of* 8×8 *elements at the 2 cm wavelength (right).*

and manufacturing a model "terrace" array (Khaikin et al., 2000). Arrays of "terrace" design can be employed in radio telescopes which are paraboloids of rotation. Axially symmetric designs of these arrays with the number of elements of 8×8 can be used in the focal region of parabolic mirrors in the range up to 30 GHz. With the number of elements of 3×3 and 4×4 they have a certain advantage over the arrays all elements of which are arranged in one plane since the "terrace" arrangement of the elements makes it possible to get a multibeam BP with the same level of signal in all beams.

References

Bird T., 1994, IEEE Antennas & Propagation Society Symp., Seattle, June, 1994

Berlin A.B., et al., 2000, Transaction of A&Ap., in press

Erickson N.K., Goldsmith P.F., Novak G.,Viscuso P.J., Erickson R.B. and Predmore, 1992, IEEE Trans., Microwave Theory Tech., MTT-40, 1

Esepkina N.A., Bahvalov N.S., Vasil'ev B.A., Vasil'eva L.G., Vodovatov I.A., Temirova A.V., 1980, Astrofiz. Issled. (Izv.SAO), **12**, 106

Esepkina N.A., Bahvalov N.S., Vasil'ev B.A., Vasil'eva L.G., Temirova A.V., 1982, Astrofiz. Issled. (Izv.SAO), **15**, 151

Esepkina N.A., Kajdanovskij N.L., Kuznetsov B.G., Kuznetsova G.V., Khaikin S.Eh., 1961, Radiotekhnika i elektronika, VI, No. **12**, 1947

Esepkina N.A., Kruglov S.K., Molodyakov S.A., Khaikin V.B., 2000, Transaction of A&Ap., **19**, No.3–4, 616

Herrmann R., Magun A., Costa J.,Correia E., Kaufman P., 1992, Solar Physics, **142**, 157

Kajdanovskij N.L., 1980, Astrofiz. Issled. (Izv.SAO), **12**, 103

Khaikin V.B., Majorova E.K., Shifman R.G., 1998, Proceed. of 2-nd ESA Workshop on Millimetre Wave Technology and Applications, Espoo, Finland, 1998

Khaikin S.E., Kajdanovskij N.L., Parijskij Yu.N., Esepkina N.A., 1972, Izv. GAO, **188**, 3

Khaikin V.B., Majorova E.K., Parijskij Yu.N., et al., 1999, Proceed. of Intern. Conf. "Perspective on radioastronomy: technologies for large antenna arrays", Dwingeloo, the Netherlands, April, 1999, 171

Korzhavin A.N., 1979, Astrofiz. Issled. (Izv.SAO), **11**, 170

Majorova E.K., Khaikin V.B., 1999, Bull. Spec. Astro-

phys. Obs., **48**, 133.
Parijskij Yu.N. et al., 1998, "Park Ages" of the Universe. NATO ASI series, **511**, 433.
Payne J.M., 1988, Rec.Sci.Instrum, **59**, 9, 1911
Pinchuk G.A., Majorova E.K., et al., 1995, Proceed. of NRAO workshop, A.S.P. Conf. series, **75**
Smits F.M., Smolders A.B., 1998, Proceed. of XXI Antenna Workshop on Antenna Array technologies, ESA IESTEC, Noordwijn.
Sutton E.C., 1984, Astrophys.J.Lett., **283**, No. 2, 41